Enabling Multi-Spot Wireless Power Transmission via Pulsed FDA for Simultaneous Dislocated Charging

Published Version:
Fazzini, E., Tiberi, T., Costanzo, A., Masotti, D. (2024). Enabling Multi-Spot Wireless Power Transmission via Pulsed FDA for Simultaneous Dislocated Charging. IEEE ANTENNAS AND WIRELESS PROPAGATION LETTERS, 23(11), 3847-3851 [10.1109/lawp.2024.3424222].

Availability:
This version is available at: https://hdl.handle.net/11585/996028 since: 2025-01-21

Published:

DOI: http://doi.org/10.1109/lawp.2024.3424222

Enabling Multi-Spot Wireless Power Transmission via Pulsed FDA for Simultaneous Dislocated Charging

Enrico Fazzini, *Graduate Student Member, IEEE*, Tommaso Tiberi, *Graduate Student Member, IEEE*, Alessandra Costanzo, *Fellow, IEEE*, and Diego Masotti, *Senior Member, IEEE*

***Abstract*— In this work the beam steering capability of pulsed frequency diverse arrays (pulsed FDAs) is analyzed and experimentally validated for the wireless energization of battery-less sensors randomly placed in a digitalized environment. The measurements, carried out for a 4-finger planar array operating at 1.9 GHz, show how it is possible to illuminate different regions of space "almost" simultaneously, by periodically selecting the *a priori* known raising time instants of the control pulses of the array excitations. The multi-sine generated signal is used as the input of a rectifying circuit, designed to face with the pulsed nature of the excitation. The simulated results demonstrate the feasibility of the envisaged powering system, where the outstanding reconfigurable capabilities of a pulsed FDA, as smart power source, guarantee RF-to-dc conversion efficiencies comparable to the standard continuous wave (CW) case.**

***Index Terms*— Frequency diverse arrays, wireless power transfer (WPT), beam steering.**

I. Introduction

In recent years frequency diverse arrays (FDAs) have gained interest in scientific community for their unique properties: the radiation mechanism, based on the intermodulation of signals at slightly different frequencies, each one radiated by an array's element, allows to obtain a time-range-angle dependent radiation pattern [1].

Initially exploited for radar applications [2],[3], FDAs have then been used as a smart radiating architecture for wireless power transfer (WPT) purposes [4],[5]. Several configurations have been proposed for enhancing the focusing capability of FDA radiation, by optimizing the radiating topology [6],[7],[8] or the frequency distribution rules [9],[10],[11]. Additionally, time-based techniques, such as the pulsed FDA, have been proposed in [12],[13], for obtaining agile and low-cost beam steering capability, by introducing RF switches, thus getting rid of expensive phase-shifters and the related cumbersome embedding networks.

Manuscript submitted on 27 March 2024.
This work was partly funded by the Italian Ministry of Education, University and Research (MIUR) within the framework of the PRIN 2022-INSIDE-NEXT ("Indoor Smart Illuminator for Device Energization and Next-generation communications") and partly by the European Union through the Italian National Recovery and Resilience Plan (NRRP) of Next Generation EU, partnership on "Telecommunications of the Future" (Program "RESTART") under Grant PE00000001.
Enrico Fazzini, Tommaso Tiberi, Alessandra Costanzo, and Diego Masotti are with DEI, Alma Mater Studiorum Università di Bologna, Bologna, 40136, Italy. (e-mail: enrico.fazzini2@unibo.it, tommaso.tiberi@unibo.it, alessandra.costanzo@unibo.it, diego.masotti@unibo.it).

In this work, the pulsed FDA agile beam steering feature is exploited for powering applications: the theoretical approach is presented and experimentally validated by means of a linear array, with a linearly increasing frequency offset. For the abovementioned purposes, the best obtained radiating topology is a 4-finger, series-fed FDA, offering a wide scanning range, in the plane where the frequency diversity is applied, and a boosted directivity in the orthogonal one. The effectiveness of the realized smart RF radiator is finally verified through a careful comparison of rectification performance on the receiver side, under different excitation conditions: standard CW, standard (not pulsed) FDA, and pulsed FDA with different pulse shapes. The numerical optimization, carried out in the available power range $[-30 \div -5]\ dBm$, shows that the pulsed FDA is slightly less effective than a standard phased array (PA) using CW excitations in the lower power range, but it is more suitable when RF power higher than -14 dBm is available, especially if triangular pulses are adopted for modulating the continuous FDA signal. This offers an interesting step forward to investigate the feasibility of a novel far-field WPT system, and to assess whether the pulsed FDA can be helpful for this purpose.

II. Pulsed FDA Model and Performance

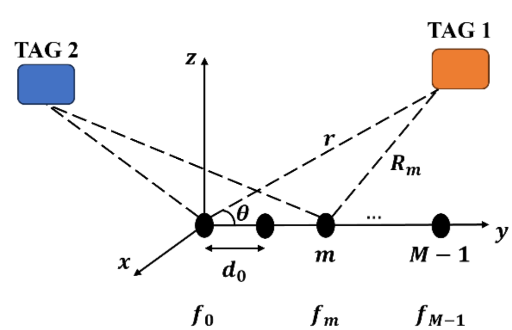

Fig. 1. Sketch of pulsed FDA for WPT applications.

Let us consider an array of M isotropic elements aligned along the y-axis, equally spaced of $d_0 = \lambda_0/2$, (λ_0 is the wavelength in vacuum), and with linear frequency distribution $f_m = f_0 + m\Delta f$, as shown in Fig. 1, whose purpose is to illuminate randomly distributed battery-less tags. The standard frequency diversity rule has been considered: f_0 is the operating frequency of the first element of the array ($m = 0$), and a linear progressive frequency offset Δf is introduced among consecutive elements. The pulsed signal radiated by the m^{th} element can be represented as:

$$x_m(t) = x_p(t - \tau) \cdot \exp(j2\pi f_m t) \quad (1)$$

where x_p is a periodic pulse of period $T_p = 1/\Delta f$ and duration $T_{on} = 20\,ns$, modulating the RF continuous wave (CW). Note that the pulse periodicity has been set equal to the time periodicity of the FDA radiation pattern ($1/\Delta f$). Even though this choice is not mandatory, it allows to univocally select the direction(s) of radiation, obtaining a full beam-steering control. The total signal transmitted by the array in a generic far field position $P(r, \theta, \varphi)$ at distance $R_m \approx r - md_0 sin\theta sin\varphi$ can be cast:

$$x(t) = \sum_{m=0}^{M-1} x_p\left(t - \tau - \frac{R_m}{c}\right) \cdot \exp\left(j2\pi f_m\left(t - \frac{R_m}{c}\right)\right) \quad (2)$$

By pulsing each transmitting element allows to obtain an unprecedented beam steering capability with no need for expensive phase-shifters, as for PA control. In fact, the combination of pulsed FDA with the linear increasing frequency offsets allows to replace the typical shape of the beam pattern (BP) vs. θ (S-shape) [1] with confined spots. Within one period, the spots pointing direction can be defined by properly setting the duty cycle and the delay τ of the pulse. This capability, as well as the harmonic generation due to the periodic time control of the excitation, can be profitably exploited for WPT purpose, provided that the antennas involved both in transmission and in reception are wideband enough to ensure in-band harmonic radiation, thus avoiding excessive out-of-band power losses, as was demonstrated for the first time in [14]. However, in [14] the system performance was evaluated through a frequency domain analysis only, deriving the most suitable set-up, in terms of pulse parameters, for WPT scenarios. A different study is here presented, focusing on the level of reconfigurability of the pulsed FDA and showing the agile beamforming capabilities achievable by a pulsed control of the FDA beam pattern.

Thus, the purpose of this section is to demonstrate the single- and multi-beam control of pulsed FDA exploiting standard rectangular pulses. The single beam is obtained when the delayed pulse (with delay τ) is raised once in a period, while multiple beams are obtained by introducing multiple pulses (with delay τ_i) in one period. The a-priori known (τ, θ) law [15] allows to select the pointing direction(s): in fact, given the standard FDA beam pattern (CW regime), by varying the pulse delay τ, a precise radiation direction is selected [14], where a confined spot centered around a user-defined θ direction is obtained.

The generic pulsed FDA control waveform can then be written as the sum of I pulses, each one composed of N_h harmonics, with the same pulse repetition frequency $F_p = \frac{1}{T_p}$ and different delay τ_i:

$$x_p(t) = \sum_{i=0}^{I-1} \sum_{h=-N_h}^{N_h} C_h^i \exp(j2\pi h F_p(t - \tau_i)) \quad (3)$$

where C_h^i are the complex harmonic coefficients of the i^{th} pulse. When a rectangular pulse is adopted, these coefficients are given by $C_h^i = A_i \cdot d_i \cdot sinc(h \cdot d_i)$, where A_i and d_i are the pulse amplitude and duty cycle, respectively. To understand the modified pulsed FDA capabilities, the normalized received multi-harmonic BP behavior, (i.e. the squared magnitude of the received signal) vs. θ of a linear array, is computed in the plane where the frequency diversity is applied (yz-plane in Fig. 1, called diversity plane in the following). For the present case the linear array consists of $M = 8$ ideal isotropic elements, operating at $f_0 = 1.9\,GHz$, and $\Delta f = 5\,MHz$. The patterns are plotted in Fig. 2, for different pulse numbers and a duty cycle equal to 0.1. For the sake of brevity, it is just worth mentioning the impact of the duty cycle on the illuminated spot dimension (i.e., the θ range covered during the ON-time), and on the power loss: the lower the duty cycle, the higher are the accuracy and the losses. While a careful analysis of the choice of the system parameters, to obtain the best trade-off between radiation accuracy and harmonic losses, has been carried out in [14]. This work aims at demonstrating the radiating properties of the pulsed FDA under various control sequences, highlighting the great agility of this proposed transmitting architecture and at validating the concept experimentally.

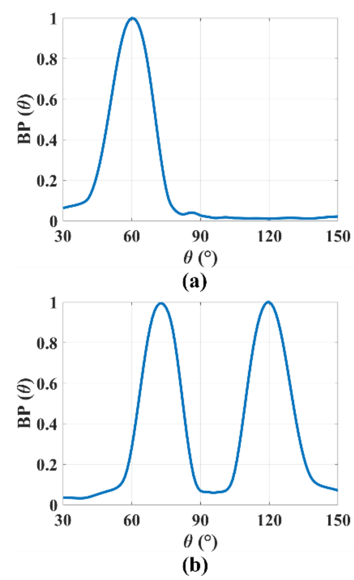

Fig. 2. Normalized multi-harmonic BP in the yz-plane (a) for I = 1, (b) for I = 2.

In Fig. 2(a), by setting $\tau = 50\,ns$, the system is able to periodically illuminate around $\theta = 60°$ with a beam whose shape depends both on the number of array elements and the duty cycle value; while Fig. 2(b) shows the capability of the system to almost simultaneously illuminate two regions (around $\theta = 70°$ and $\theta = 120°$) by adopting two delayed pulses with $\tau_1 = 30\,ns$ and $\tau_2 = 150\,ns$, respectively. To the authors' opinion, this behavior highlights the superiority of pulsed FDA over other radiating architectures, such as PA or time modulated arrays (TMA). This can be also inferred by considering the constraint that the pulsed control given by the summation of two delayed pulses must fulfill:

$$\tau_1 + \tau_2 \leq \frac{1}{\Delta f} \quad (4)$$

Therefore, the two (or more) delays may be either complementary (case i) or not (case ii) with respect to the FDA time periodicity ($1/\Delta f$), i.e. the sum of the delays may be even lower than or equal to $1/\Delta f$. In this second scenario, the overall pulsed signal is processed as a single pulse with halved periodicity, i.e. with double repetition frequency. Therefore, the harmonics distribution varies in the two cases: however, the spectral analysis in [14], has proven that there is no difference in terms of power losses and the overall performance remain the same. Consequently, one can say that pulsed FDAs have no restriction on the multi-beam pointing directions, being both the asymmetric (case ii)) and symmetric (case i)) choices possible without any issue. This fact is the added value of the proposed radiating architecture if compared, for instance, to TMA where symmetric radiation through the sideband harmonics is mandatory [16], except for the case of complex feeding strategies exploitation [17]. Moreover, a much reduced hardware complexity and a high level of reconfigurability are important requirements for WPT, and those aspects are essential advantages of the pulsed FDA with respect to other solutions, such as those based on Butler Matrix or Rotman Lens. Indeed they still allow multi-beam capabilities, and despite their easier signal excitations (no superior harmonics to be handled), a much more complex and expensive feeding networks adopting distributed hybrid couplers and phase shifters is required [18]. A comparison between the proposed pulsed FDA and other solutions in the literature is summarised in Table I.

Table I

Architecture	Multi-beam capability	Hardware implementation	Pattern reconfigurability	Signal excitations
Rotman Lens [18]	Yes	Complex feeding network	Moderate	Single carrier
Butler Matrix [18]	Yes	Hybrid couplers and phase shifters	Moderate	Single carrier
Time Modulated Arrays [16]	Only in symmetric directions	Switch at each antenna port	High	Single carrier + superior harmonics
Pulsed FDA (this work)	Yes	Multi-tone generation + switch at each antenna port	High	Multi-carrier + superior harmonics

III. Measurements of Pulsed FDA

When realistic antenna topologies are involved, the illuminated θ-sector in the diversity plane is reduced due to practical impairments. This phenomenon introduces some limitations and the entire 180-degree span in front of the array is not available anymore. To monitor the actual angular span, a figure-of-merit able to quantify the scanning region of the FDAs (SR_{FDA}) can be defined as follows:

$$SR_{FDA} = \{\theta: [0°, 180°] |\, BP(\theta) - BP_{MAX} \geq -3\ dB\} \quad (5)$$

This parameter defines the θ-range that can be periodically spanned by the FDAs beam pattern, without exceeding a 3 dB difference with respect to its maximum BP_{MAX}. Indeed, a pulsed FDA system made by ideal isotropic elements is able to scan the entire half space in front of the transmitter by moving along the S-shape of its beam pattern. While, with its realistic implementation the SR_{FDA} range is strongly reduced, due to the fact that real radiators (e.g. patch antennas) illuminate a limited angular sector only. To mitigate this problem, the series-fed array has been chosen as a valuable topology since it is able to achieve a rather wide SR_{FDA}. This array architecture has been designed and exploited to carry out the experimental validation of the pulsed FDAs, shown in this section.

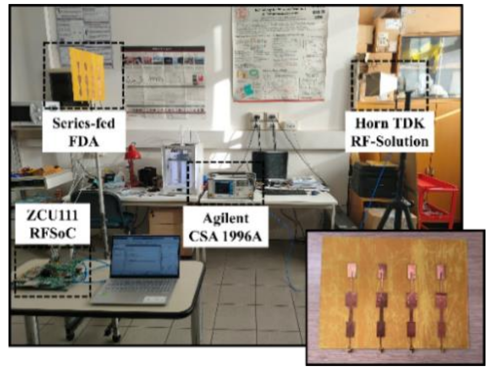

Fig. 3. Measurement set-up and zoomed view of the adopted multi-finger transmitting array.

To validate single-beam and multi-beam radiation capabilities of the pulsed FDA, measurements with a 4-finger series-fed FDA (view inset in Fig. 3), realized on a 1-mm-thick ISOLA DE104 substrate ($\varepsilon_r = 4.37$, $tan\delta = 0.022$) operating at 1.9 GHz, are presented. Each finger consists of a series-fed array of 3 patches, each one tuned to properly cover a wide bandwidth of approximately 100 MHz, thus to profitably radiate most of the harmonics produced by the pulsed excitation, hence minimizing the power loss [14]. The array shows a SR_{FDA} of approximately 70°. The performance, in terms of both bandwidth and scanning range exceeds those obtained by a simpler linear array of patches. The measurement set-up is shown in Fig. 3, in which a software defined radio (Xilinx ZCU111) is used to generate the multi-channel pulsed RF excitations.

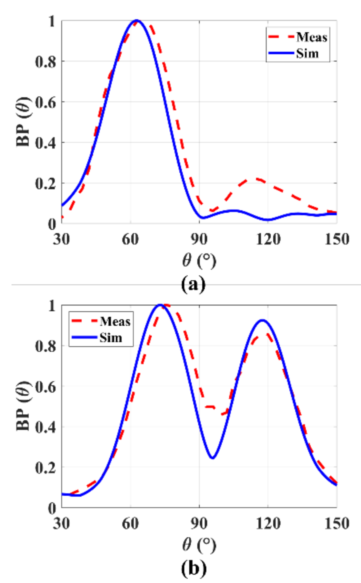

Fig. 4. Measurements vs simulations of the normalized multi-harmonic BP in the y-z plane for (a) I = 1 and (b) I = 2.

Figs. 4 show the predicted and experimental results using the radiating array of Fig. 3, on the overall they are consistent with those in Figs. 2. A delay $\tau = 50\ ns$ selects a maximum in the direction $\theta = 60°$ (Fig. 4(a)), while in Fig. 4(b) the multi-beam capability is retrieved exploiting two delays of 30 ns and 150 ns, respectively, providing simultaneous radiation at $\theta = 70°$ and $\theta = 120°$, for each time-period. Any pointing direction inside the SR_{FDA} can be easily selected by adjusting the τ_i parameters. It is noteworthy that the single- and multi-beam radiation of pulsed FDA have been experimentally validated for the first time in this work, being the great majority of the literature on FDA purely theoretical.

IV. FDA Rectifier Design

Once the unique dynamic radiation mechanism of the pulsed FDA is demonstrated, let's verify its effectiveness in WPT applications, by considering the behaviour of a rectenna located in the illuminated locations. For this purpose, a Harmonic Balance (HB) optimization [19] of a rectenna whose equivalent circuit is shown in Fig. 5 is performed, by adopting the actual input waveforms as its excitations.

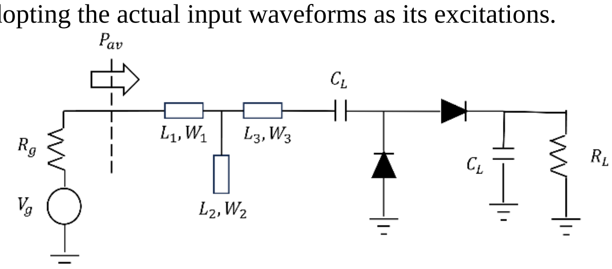

Fig. 5. Layout of the rectifier circuit of the receiving TAG.

The circuit is realized on a 1.5-mm-thick ISOLA FR408HR ($\varepsilon_r = 3.68$, $tan\delta = 0.0092$). The same material resulted to be feasible for the direct connecting the receiving antenna to the rectifier.

The HB optimization of the RF-to-dc efficiency (η_{RF-DC}) has been performed over an available power (P_{av}) range of $[-30 \div -5]\ dBm$. A single-tone CW, a 4-tone CW FDA, and a 4-tone pulsed FDA are compared over a bandwidth of 100 MHz. For each case the optimum set of the design parameters is reported in Table II. The input line is fixed ($W_1 = 3.23\ mm$, to match the antenna 50-Ω impedance, and $L_1 = 3W_1$); the capacitors are equal to 1 nF and the diodes are Skyworks SMS7630-079LF.

The simulation results are summarized in Figs 6, of course, for a given P_{av}, the highest received peak-to-average power ratio (PAPR) is obtained by the pulsed FDA. As can be evinced from Fig. 6(a), the pulsed FDA rectifier excitation results in a slightly worse efficiency, in the lower power range.

Table II

Config.	$L_2\ (mm)$	$W_2\ (mm)$	$L_3\ (mm)$	$W_3\ (mm)$	$R_L\ (k\Omega)$
1-tone CW	18.3	5	10.8	0.3	11.2
4-tone CW FDA	17.1	5	11	0.3	16.4
4-tone pulsed FDA	14.3	4.65	11.5	0.3	26.7

For P_{av} exceeds -14 dBm, the pulsed FDA system outperforms both the 4-tones CW FDA and single tone CW. Additionally, the pulsed FDA system allows flexibility with respect to the pulse waveforms. Finally, by exploiting the pulsed FDA HB analysis, with varying the shape of the control waveform [14], it is interesting to look at the rectifying performance in the presence of different pulses modulating the RF signals. As an example, in Fig. 6(b) a slight (but increasing with the power level) improvement is achieved by resorting to triangular pulsed waveforms, which are also convenient to minimize the power loss in transmission [14] and for the illuminated spot definition [20].

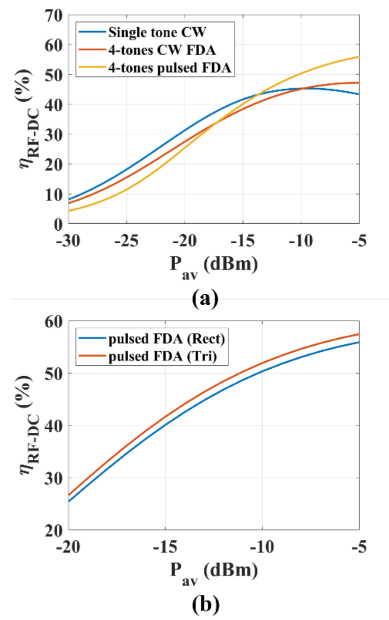

Fig. 6. (a) RF-to-dc efficiency for different input excitations and (b) for different input pulse shapes for pulsed FDA.

V. Conclusion

An analytical and experimental characterization of the flexible beam steering capability of pulsed FDAs has been provided for the first time. The use of multifrequency switched excitations, applied to the FDA scheme, allows to beaming power in different directions simultaneously, with the possibility of creating, dynamically in real-time, single- or multi-beam pattern, suitable for the smart energization of battery-less sensors. The high PAPR pulsed multi-tone powering signal is also fruitful at the rectenna side, especially if medium power level (> -14 dBm) is available. The RF-to-dc efficiency can be further boosted if non-standard pulses are used, to drive switched excitation, such as triangular waveforms. Future works will be devoted to the rectenna realization and the study of excitation sequences with the most appropriate harmonic content for rectification purposes.

References

[1] P. Antonik, M. C. Wicks, H. D. Griffiths, and C. J. Baker, "Frequency diverse array radars," in *2006 IEEE Conference on Radar*, Verona, NY, USA, 2006, pp. *3* pp.-..

[2] W. -Q. Wang and H. C. So, "Transmit Subaperturing for Range and Angle Estimation in Frequency Diverse Array Radar," *IEEE Trans. Signal Process.*, vol. 62, no. 8, pp. 2000-2011, April 2014.

[3] J. Xu, G. Liao, S. Zhu, L. Huang and H. C. So, "Joint Range and Angle Estimation Using MIMO Radar With Frequency Diverse Array," *IEEE Trans. Signal Process.*, vol. 63, no. 13, pp. 3396-3410, July 2015.

[4] A. Yao, N. Anselmi and P. Rocca, "A multi-carrier frequency diverse array design method for wireless power transmission," in *2018 12th European Conference on Antennas and Propagation (EuCAP)*, London, UK, 2018, pp. 1-4.

[5] A. -M. Yao, P. Rocca, W. Wu and A. Massa, “On the design of frequency diverse arrays for wireless power transmission,” in *2017 11th European Conference on Antennas and Propagation (EUCAP)*, Paris, France, 2017, pp. 900-903.

[6] A. M. Jones and B. D. Rigling, "Planar frequency diverse array receiver architecture," in *2012 IEEE Radar Conference*, Atlanta, GA, USA, 2012, pp. 0145-0150.

[7] A. Akkoç, E. Afacan and E. Yazgan, “Investigation of Planar Frequency Diverse Array Antenna in Concentric Circular Geometry,” in *2019 11th International Conference on Electrical and Electronics Engineering (ELECO)*, Bursa, Turkey, 2019, pp. 651-654.

[8] E. Fazzini, A. Costanzo and D. Masotti, "A New Wheel-Spoke Transmitter for Efficient WPT Based on Frequency Diversity," in *2022 52nd European Microwave Conference (EuMC)*, Milan, Italy, 2022, pp. 576-579.

[9] A. Basit, I. M. Qureshi, W. Khan, S. u. Rehman and M. M. Khan, "Beam Pattern Synthesis for an FDA Radar with Hamming Window-Based Nonuniform Frequency Offset," *IEEE Antennas Wireless Propag. Lett.*, vol. 16, pp. 2283-2286, June 2017.

[10] Y. Liao, W. -Q. Wang and Z. Zheng, “Frequency Diverse Array Beampattern Synthesis Using Symmetrical Logarithmic Frequency Offsets for Target Indication,” *IEEE Trans. Antennas and Propag.*, vol. 67, no. 5, pp. 3505-3509, May 2019.

[11] W. Xu, L. Zhang, H. Bi, P. Huang and W. Tan, "FDA Beampattern Synthesis With Both Nonuniform Frequency Offset and Array Spacing," *IEEE Antennas Wireless Propag. Lett.*, vol. 20, no. 12, pp. 2354-2358, Dec. 2021.

[12] Y. Xu, X. Shi, J. Xu and P. Li, “Range-Angle-Dependent Beamforming of Pulsed Frequency Diverse Array,” *IEEE Trans. Antennas and Propag.*, vol. 63, no. 7, pp. 3262-3267, July 2015.

[13] E. Fazzini, A. Costanzo and D. Masotti, "Ranging On-Demand Microwave Power Transfer in Real-Time," *IEEE Microw. Wireless Comp. Lett.*, vol. 31, no. 6, pp. 791-793, June 2021.

[14] T. Tiberi, E. Fazzini, A. Costanzo and D. Masotti, "Exploitation of Harmonic Generation in Time-Controlled Frequency-Diverse Arrays for WPT," *IEEE Trans. Antennas and Propag.*, vol. 72, no. 1, pp. 497-505, Jan. 2024.

[15] Jingjing Huang, Kin-Fai Tong and C. J. Baker, “Frequency diverse array with beam scanning feature,” in *2008 IEEE Antennas and Propagation Society International Symposium*, San Diego, CA, USA, 2008, pp. 1-4.

[16] D. Masotti, A. Costanzo, M. Del Prete and V. Rizzoli, "Time-Modulation of Linear Arrays for Real-Time Reconfigurable Wireless Power Transmission," *IEEE Trans. Microw. Theory Techn.*, vol. 64, no. 2, pp. 331-342, Feb. 2016.

[17] A. -M. Yao, W. Wu and D. -G. Fang, "Single-Sideband Time-Modulated Phased Array," *IEEE Trans. Antennas and Propag.*, vol. 63, no. 5, pp. 1957-1968, May 2015.

[18] N. Jastram and D. S. Filipovic, "Wideband multibeam millimeter wave arrays," in *2014 IEEE Antennas and Propagation Society International Symposium (APSURSI)*, Memphis, TN, USA, 2014, pp. 741-742.

[19] S. Yu, F. Cheng, C. Gu, C. Wang and K. Huang, “Compact and Efficient Broadband Rectifier Using T-type Matching Network,” *IEEE Microw. Wireless Comp. Lett.*, vol. 32, no. 6, pp. 587-590, June 2022.

[20] E. Fazzini, T. Tiberi, A. Costanzo and D. Masotti, "Advanced Reconfigurability of Frequency-diverse Radiators for both Localization and Powering," in *2023 17th European Conference on Antennas and Propagation (EuCAP)*, Florence, Italy, 2023, pp. 1-4.